

Development of chromia forming Mo-W-Cr alloys: synthesis and characterization

S. DILIBERTO, O. KESSLER, C. RAPIN, P. STEINMETZ, P. BERTHOD
*Laboratoire de Chimie du Solide Minéral, UMR CNRS 7555, Université Henri Poincaré,
BP 239, 54506 Vandoeuvre, France*
E-mail: pierre.steinmetz@lscsm.uhp-nancy.fr

The sintering process and microstructural characteristics of tungsten-based and molybdenum-based alloys containing chromium and group VIII metals as sintering agents have been investigated. The influences of the alloy composition, the nature of the sintering agent and the synthesis process on the microstructure and microhardness of these materials have been studied. Homogeneous alloys can be obtained with palladium or nickel as the sintering agent. The mechanisms are totally different with these two metals. In the case of nickel, diffusion of the refractory metals through a nickel layer is responsible for the densification of the alloys, whereas with palladium, a CrPd liquid phase at the grain boundaries leads to homogeneous sintering. Formation of the CrPd phase is directly dependent on the chromium content which influences the solubility of palladium in the MoW matrix. Consequently, a low chromium content leads to a high CrPd content, and to an increase in the grain size. On the contrary, with a nickel sintering agent, a high Ni content leads to an increase in thickness of the interdiffusion layer and thus a decrease in the grain size. Stresses generated by uniaxial sintering and mechanical alloying are not released during the annealing sequence and contribute to increase the microhardness of the alloys. Microhardness is also a strong function of the tungsten content.

© 2002 Kluwer Academic Publishers

1. Introduction

Many industrial applications require high-performance materials with good mechanical properties and high resistance to oxidation/corrosion at high temperatures. This is especially true in the glass industry, where metallic or ceramic materials suffer from high temperature oxidation and corrosion by molten glass at temperatures up to 1200°C or higher. In most applications, good mechanical properties are also necessary.

As in other industrial fields, glass melting processes is evolving towards higher temperatures than those used classically. For example, due to changes in glass compositions used to make insulation materials, temperature targets for fiberglass processing can be as high as 1300°C. In this case, iron-, nickel- or cobalt-based alloys cannot be used, due to their drastic loss of mechanical properties above 1200°C.

Because of the need for high temperature mechanical properties and resistance to molten glass corrosion, the development of refractory alloys based on tungsten and/or molybdenum seems to be relevant. But the oxidation resistance of these metals is very bad, so that alloying with elements which form protective oxide layers is a necessity. Among the elements which can be used for this purpose, aluminium or silicon must be excluded, because their oxides are

very soluble in molten glass. Chromium is preferred, since its oxide has a low solubility in most acidic glasses.

In the past, some authors have studied Mo- and/or W based alloys containing chromium. Evans [1] was the first to describe a method of preparation of such alloys, with sintering of a powder mixture of the constituent elements containing an activating agent (palladium). Dzykovitch *et al.* [2] confirmed later that palladium is necessary to activate interdiffusion in the W-Cr binary system, probably because it temporarily forms limited quantities of a molten CrPd phase. Lee and Simkovich [3–6] have studied some compositions of MoCrPd and MoWCrPd alloys and showed that the combination of tungsten and molybdenum offers the best performance in high temperature oxidation. They claimed that the Cr₁₉Mo₄₀W₄₀Pd₁ alloy displays excellent oxidation behaviour.

Nothing has been done on chromium rich alloys, nor on the influence of the W/Mo ratio or the nature of the sintering agent. These parameters, and also the methods for preparing chromium rich Mo-W-Cr alloys, have been studied here, with the main objective to find alloy compositions which could satisfy the requirements of resistance to high temperature oxidation/corrosion and good mechanical properties.

TABLE I Types of metallic powder used

Elements	Origin	Granulometry	Purity
Chromium	Cerac	-325 mesh	99.6%
Molybdenum	Cerac	-325 mesh	99.9%
Tungsten	Cerac	-325 mesh	99.5%
Palladium	Jonhson Matthey	1-1.5 μm	99.95%
Nickel	Cerac	-325 mesh	99.9%
Ruthenium	Jonhson Matthey	Sponge	>99%

2. Experimental

2.1. Materials

Metal powders with characteristic given in Table I were supplied by CERAC*. In order to limit the diffusion time, only micronic size powders were used.

2.2. Methods of elaboration

Preliminary to sintering, the elemental powders were weighed, then blended to obtain a homogeneous mixture. Most blending was done manually in an agate mortar, but sometimes mechanical alloying was carried out. In this latter case, a planetary ball mill (FRITSCH model pulverisette 5) was used; the corresponding experimental conditions are described later.

Two sintering methods were used: natural sintering and sintering with uniaxial pressure assistance.

For natural sintering, the powders were hand-mixed using a mortar and pestle for 30 min. The powder mixture was then put into an uniaxial die and hydraulically pressed to 600 MPa at room temperature. The resulting cylindrical specimens were approximately 13 mm in diameter and 5 mm high. The pressed samples were heated for 2 hours at 1370°C under an H₂ atmosphere (commercial H₂), then for 22 hours at 1420°C under an argon atmosphere.

High pressure sintering was carried out using a high temperature furnace equipped with a 10 ton uniaxial press. The metal powders were previously mixed in an agate mortar or prepared by mechanical alloying, and then introduced in a graphite die (Fig. 1b). To avoid carburization of the powders, a papyex[†] sheet covered with boron nitride was inserted between the matrix and the powders. BN acts as barrier for diffusion of carbon. The experimental schedule is shown in Fig. 1a. for effective pressure and temperature during sintering.

For mechanical alloying, a planetary ball mill was operated at 350 rpm. The elemental powders and steel balls were loaded into a steel container closed under an argon atmosphere to limit oxidation. All mechanical alloying processing was done for 3 hours, with a mass ratio $M_{\text{balls}}/M_{\text{powder}}$ equal to 10.

2.3. Characterisation of the samples

Mechanically alloyed powders were characterised by X-Ray diffraction (Guinier camera, Co K α). For sintered alloys, some X-Ray diffraction experiments were also done, but they were mainly characterised by microprobe analyses of cross-sections prepared by polishing

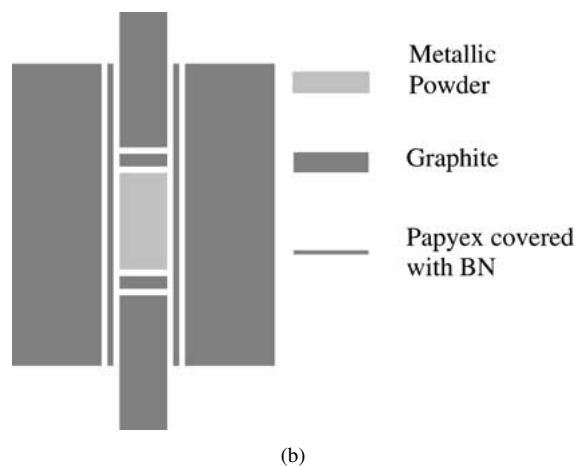
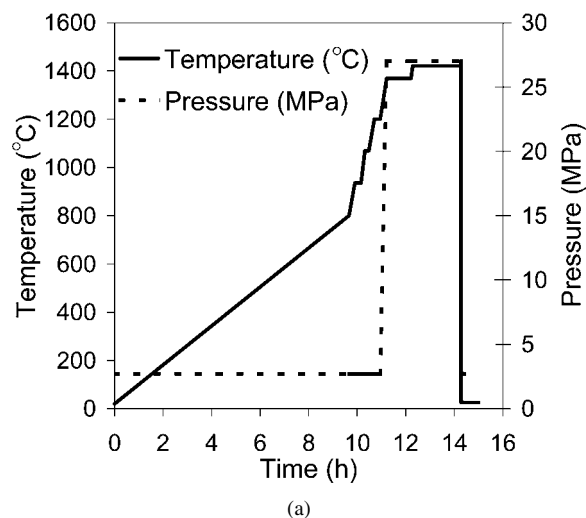


Figure 1 (a) Temperature and pressure sequences used to synthesize alloys. (b) Scheme of graphite die.

samples embedded in an epoxy resin, to 1 μm diamond paste.

Vickers microhardness measurements were carried out with a Reichert micrometer device (applied load: 100 g). Grain sizes were estimated by measuring the dimensions (in two orthogonal directions) of at least 20 grains on metallographic sections. Only maximum values were taken into account, considering the spherical approximation for grains.

The microstructure of samples was examined after repeating at least three times the following sequence of operations: 1 minute immersion in the Murakami etchant, then water, followed by ethyl alcohol cleaning and air drying.

3. Results

Several aspects of the synthesis have been studied. They are presented in the following sections. The influences of the synthesis methods and the composition on microstructure and hardness have been investigated.

3.1. Synthesis methods

The influences of the following three parameters on the resulting microstructure and physical properties of the alloys have been studied: choice of the sintering agent, mechanical alloying, and sintering method (natural or high pressure).

*Cerac incorporated: P.O. box 1178 Milwaukee, WI 53201.

[†]Carbone lorraine trade mark.

TABLE II Influence of the sintering agent on density, grain size and microhardness

Composition (weight%)	Theoretical density ($\text{g} \cdot \text{cm}^{-3}$)	Apparent density ($\text{g} \cdot \text{cm}^{-3}$)	Process	Estimated grain size (μm) $\pm 10\%$	Microhardness (Hv) $\pm 2\%$
$\text{Cr}_{39}\text{Mo}_{30}\text{W}_{30}\text{Pd}_1$	9.98	9.80	High pressure sintering	30	700
$\text{Cr}_{39}\text{Mo}_{30}\text{W}_{30}\text{Ni}_1$	9.95	9.80	High pressure sintering	75	1040
$\text{Cr}_{39}\text{Mo}_{30}\text{W}_{30}\text{Ru}_1$	9.98	9.85	Mechanical alloying + H.P. sintering	15	–

3.2. Choice of the sintering agent

From the literature, the sintering of refractory alloys containing tungsten, molybdenum and chromium, is quite difficult in the absence of a sintering agent. For example, Dzykovitch *et al.* [2] have shown that interdiffusion in the tungsten–chromium system is very slow at 1200°C when pure W and Cr are used. In the presence of palladium, interdiffusion is significantly accelerated. Corti [7] has also shown that sintering rate of tungsten is increased when limited amounts of group VIII metals are added to the initial powders, the most efficient activators being palladium and nickel. A sintering agent which can activate interdiffusion between the metallic grains of the powder mixture is thus necessary.

The preferred Group VIII metals, must satisfy two requirements: to form temporarily (a limited quantity of) a molten phase which can accelerate diffusion, and to be soluble in the alloy at the end of the sintering process, so as to avoid the presence of phases with a low liquidus temperature in the final product.

Like Corti [7], we tested palladium and nickel first. Experiments were also done with ruthenium to determine the influence of a “refractory” platinum metal as sintering activator. All experiments were done with powder mixtures prepared by manual blending, except when ruthenium was used. In this last case, the initial experiments showed that manual blending indeed led to very heterogeneous alloys: mechanical alloying has thus been used in this case.

Table II shows the grain size and hardness results obtained with a reference composition, $\text{Cr}_{39}\text{Mo}_{30}\text{W}_{30}\text{Pd}_1$. All the compositions have a body centered cubic structure and the theoretical densities can be approximated by assuming that the cell parameter follows Vegard’s law. The apparent densities were determined by picnometry. Observation of samples after sintering shows that palladium and nickel gave the best results; these alloys were homogeneous and no visible porosity was observed. The only differences observed between Pd and Ni were with grain size and hardness values which were significantly higher for sintered alloys activated with nickel.

Fig. 2a shows the typical alloy structure when Pd or Ni was used as sintering agent. Alloys are homogeneous

and no preferential grain orientation is displayed despite the applied uniaxial pressure. For the ruthenium alloy, even with use of mechanical alloying to prepare fine and homogeneous powders, the alloys obtained were very heterogeneous, as shown in Fig. 2b. Constituents are partially combined and hardness values are very inconsistent. With increasing sintering time and/or temperature, no significant improvement could be observed and the measured values have thus not been reported in Table II. Ruthenium was definitely considered as a bad sintering agent in this particular case.

The influence of the Ni or Pd content (sintering agent) has also been studied. Table III shows that when the nickel concentration was increased from 1 to 5%, the measured grain size and microhardness decreased significantly.

Fig. 3a clearly highlights a linear evolution of the grain size with the square root of the weight percent of nickel. The microhardness also decreases linearly with the nickel content (Fig. 3b).

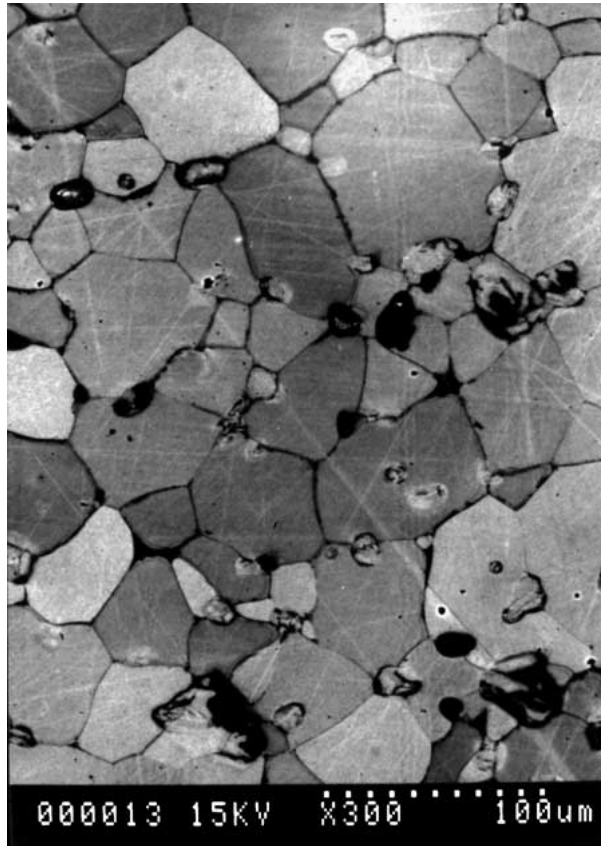
3.3. Mechanical alloying of elementary powders

Relative to the mechanical alloying conditions, only the time for powder preparation was varied, all other parameters being fixed (see previous section). After each experiment, a diffraction pattern was recorded, to observe the advance of the reaction. Fig. 4 shows the evolution with time of the X-Ray spectra recorded for the $\text{Cr}_{19}\text{Mo}_{40}\text{W}_{40}\text{Pd}_1$ alloy powder from 0 to 24 hours mechanical alloying.

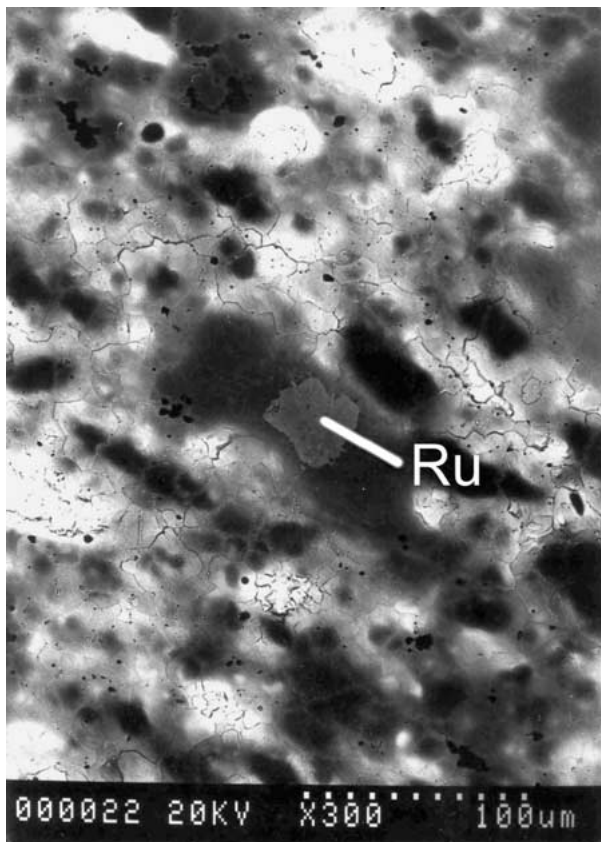
According to Fig. 4, reaction between the constituting powders is very slow, since after 24 hours milling, (110) chromium, molybdenum and tungsten diffraction peaks are still discernable, although with some difficulty in the case of Mo and W, because of the proximity of their diffraction peaks. Comparison of Figs 4c and 5 clearly shows that 24-hour mechanical alloying does not lead to complete alloying of the powders; one sharp peak is observed at $2\theta = 48.7^\circ$ for the alloy which is sintered at high temperature, whereas individual diffraction peaks of the constituent alloy elements (W, Mo and Cr) are still observed after 24-hour mechanical alloying.

TABLE III Influence of Ni level on density, grain size and microhardness

Composition (weight%)	Theoretical density ($\text{g} \cdot \text{cm}^{-3}$)	Apparent density ($\text{g} \cdot \text{cm}^{-3}$)	Process	Estimated grain size (μm) $\pm 10\%$	Microhardness (Hv) $\pm 2\%$
$\text{Cr}_{39}\text{Mo}_{30}\text{W}_{30}\text{Ni}_1$	9.95	9.90	High pressure sintering	75	1040
$\text{Cr}_{39}\text{Mo}_{29}\text{W}_{29}\text{Ni}_3$	9.88	9.85	High pressure sintering	50	888
$\text{Cr}_{39}\text{Mo}_{28}\text{W}_{28}\text{Ni}_5$	9.80	9.70	High pressure sintering	30	720

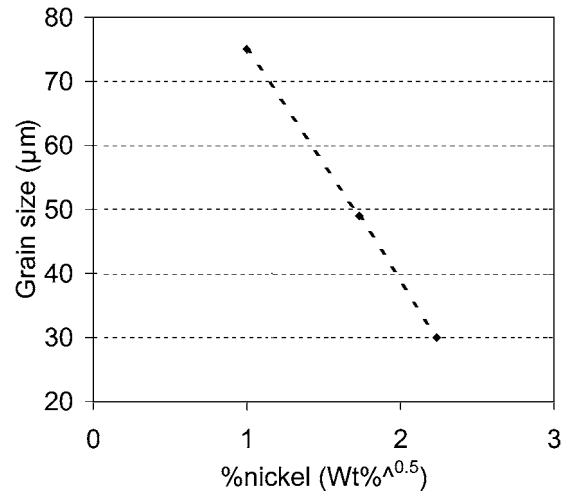


(a)

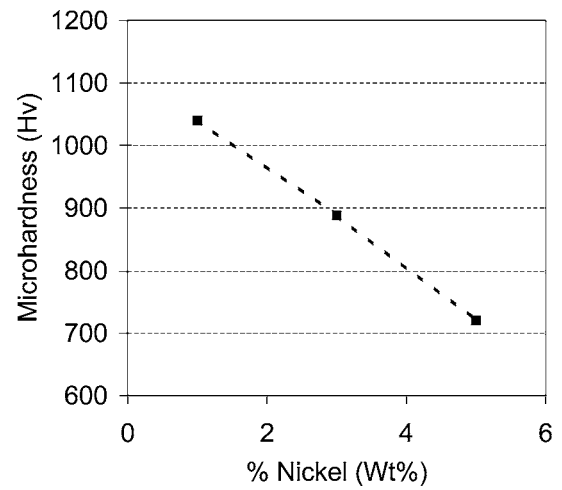


(b)

Figure 2 (a) Backscattered electron image of the $\text{Cr}_{19}\text{Mo}_{40}\text{W}_{40}\text{Pd}_1$ alloy: 1 h 1600°C and 2 h 1670°C under 27 MPa and heated at 1420°C for 2 h under H_2 and 22 h under Ar. (b) Backscattered electron image of the $\text{Cr}_{19}\text{Mo}_{40}\text{W}_{40}\text{Ru}_1$ alloy: 1 h 1600°C and 2 h 1670°C under 27 MPa and heated at 1420°C for 2 h under H_2 and 22 h under Ar.



(a)



(b)

Figure 3 (a) Grain size evolution with the square root of the Ni content. (b) Microhardness evolution with the Ni content.

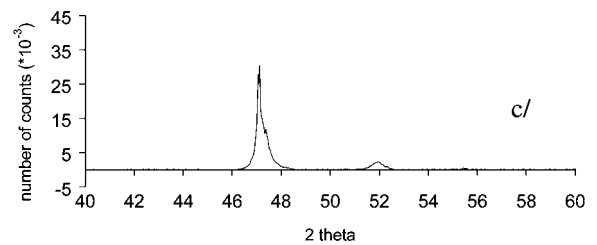
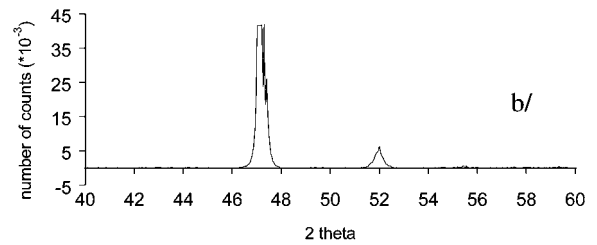
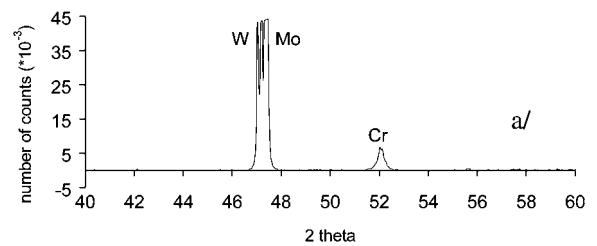


Figure 4 X-ray diffraction (Co $\text{K}\alpha$) after 0 h (a), 3 h (b) and 24 h (c) milling $\text{Cr}_{19}\text{Mo}_{40}\text{W}_{40}\text{Pd}_1$.

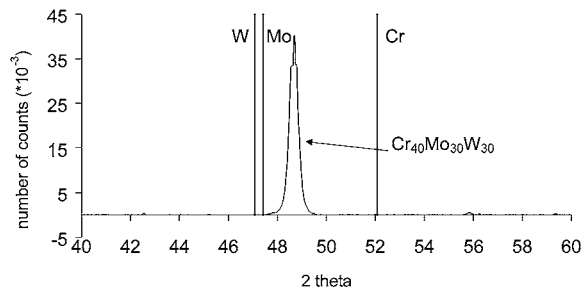


Figure 5 X-ray diffraction (Co K α) after high temperature sintering Cr₄₀Mo₃₀W₃₀.

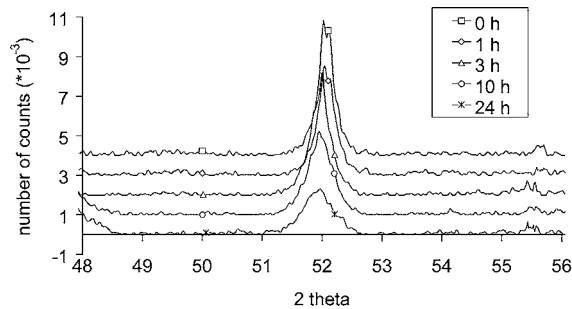


Figure 6 Chromium peak evolution with time of mechanical alloying (Co K α).

In Fig. 4, enlargement of the peaks is observed, indicating that the size of the metal grains has drastically decreased. If one looks more precisely at the chromium peak, a small evolution of its position with time of mechanical alloying is observed. A very limited reaction between chromium and the refractory metals is thus suspected. (Fig. 6). Despite this reaction, mechanical alloying is not adequate to fully alloy the elemental powders. The decrease in the grains size can however contribute to a reduction in the diffusion time during sintering.

3.4. Synthesis techniques

Three methods can be used to prepare bulk samples from powder mixtures: natural or high pressure sintering, both with hand-ground powder mixtures, and high pressure sintering with powder mixtures prepared by mechanical alloying.

Whatever the synthesis method used, all prepared alloys are homogeneous except those prepared for preliminary tests with ruthenium. The observed differences concern the density, grain size and hardness. Table IV shows how these parameters vary with the synthesis method, for the reference alloy chosen here, Cr₃₉Mo₃₀W₃₀Pd₁.

In accordance with literature data Lee and Simkovich [3–6], natural sintering leads to porous alloys. Porosity can be nearly closed with the use of high pressure sintering (27 MPa), without modification of the alloy grain size. A significant change in the hardness value is also observed when changing the sintering method, which can probably be explained by differences in density.

3.5. Alloy composition

Two CrMoWPd alloys composition parameters were studied here:

TABLE IV Influence of the method of synthesis

	Theoretical density (g · cm ⁻³)	Apparent density (g · cm ⁻³)	Estimated grain size (μm) ±10%	(Hv) ±2%
Natural sintering	9.98	8.50	30	620
High pressure sintering	9.98	9.90	30	700
Mechanical alloying + High pressure sintering	9.98	9.90	15	728

TABLE V Alloys studied with different Cr content

Composition (weight%)	Natural sintering	High pressure sintering	Mechanical alloying + high pressure sintering
Cr ₁₉ Mo ₄₀ W ₄₀ Pd ₁	*	*	
Cr ₂₄ Mo _{37.5} W _{37.5} Pd ₁	*	*	
Cr ₂₉ Mo ₃₅ W ₃₅ Pd ₁	*	*	*
Cr ₃₄ Mo _{32.5} W _{32.5} Pd ₁	*	*	*
Cr ₃₉ Mo ₃₀ W ₃₀ Pd ₁		*	*
Cr ₄₉ Mo ₂₅ W ₂₅ Pd ₁			*

- the chromium content for a Mo/W weight ratio fixed at unity
- the molybdenum/tungsten ratio, for a given chromium concentration

3.6. Influence of the chromium content

The compositions and methods of synthesis of alloys prepared for this part of the study are given in Table V. All compositions correspond to a Mo/W weight ratio fixed to 1.

Figs 7 and 8 display the dependencies of grain size and microhardness, respectively, on the chromium content and the different methods of synthesis.

A significant difference in grain size was observed between samples prepared from manually blended powders and those prepared by mechanical alloying. Fig. 7 shows indeed that bigger grain sizes are observed in the case of manual blending, compared to mechanical alloying.

Moreover, the grain size decreases with the chromium content between 19 and 39 wt% chromium, independent of the method used for powders preparation.

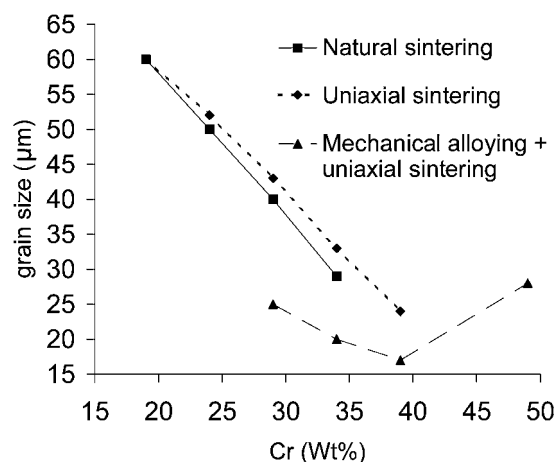


Figure 7 Influence of the method of synthesis on the grain size of the alloys.

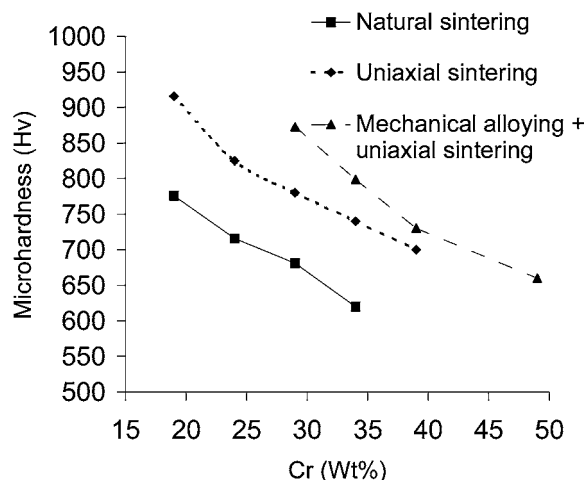


Figure 8 Evolution of microhardness versus Cr content: Influence of the synthesis method.

Higher chromium contents were studied only with ball milled powders. In this case, the grain size increases from 39 to 49 wt% Cr as seen in Fig. 7.

The dependence of the microhardness evolution with the alloy chromium content is more regular. The linear decrease has about the same slope for the different preparation techniques used. For a given composition, the lowest hardness values are observed for natural sintering, and the maximum values for mechanically alloyed powders with high pressure sintering. The difference between the two extreme values is about 200 Hv for the compositions studied.

Above 34 wt% chromium, the alloys were mono-phase, a cubic α MoWCrPd solid solution. Below 34 wt% Cr, a second phase was observed at the grain boundaries of the α matrix. Microprobe analyses have shown that this phase contains mainly chromium and palladium. (Table VI). The electronic and Pd $L\alpha$ X-Ray images showing this phase in a $Cr_{19}Mo_{40}W_{40}Pd_1$ alloy are presented in Fig. 9.

3.7. Molybdenum-tungsten ratio

The influence of the molybdenum/tungsten weight ratio was studied at constant chromium and palladium contents (39 and 1 wt%, respectively). All samples were prepared by high pressure sintering of manually blended powders. Due to the high tungsten content of some alloys, a modification of the sintering procedure was necessary, with an increase of the annealing temperature from 1400 to 1600°C (24 h).

All the alloys were homogeneous. Their compositions are given on Table VII where their grain size and hardness values are also reported. Fig. 10 displays the dependence of these two parameters on the tungsten

TABLE VI Composition of the palladium phase observed at the grains boundaries

	Chromium	Molybdenum	Palladium	Tungsten
wt%	64.31	5.4	24.52	5.77
at.%	76.54	3.62	14.82	2.02

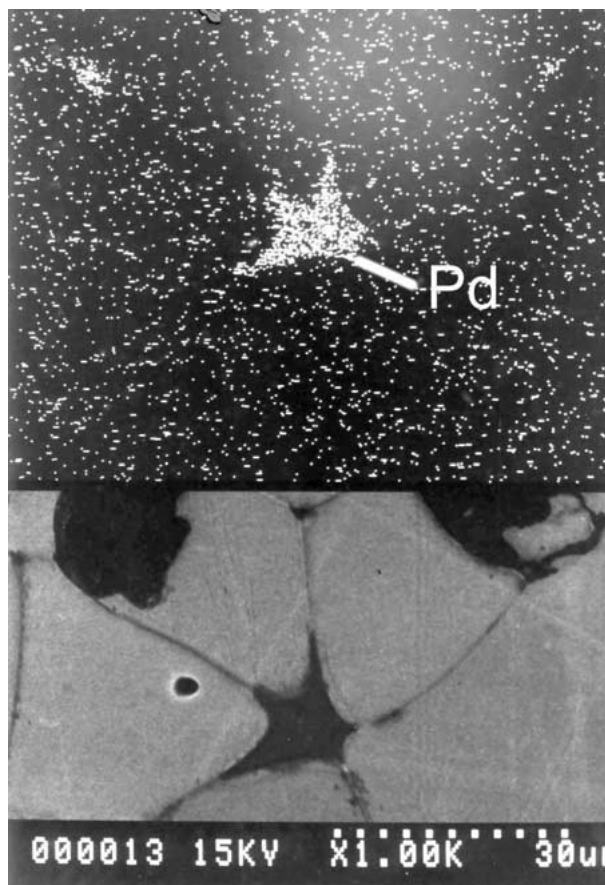


Figure 9 $Cr_{19}Mo_{40}W_{40}Pd_1$ alloys: Microstructure and Pd $L\alpha$ X-ray image.

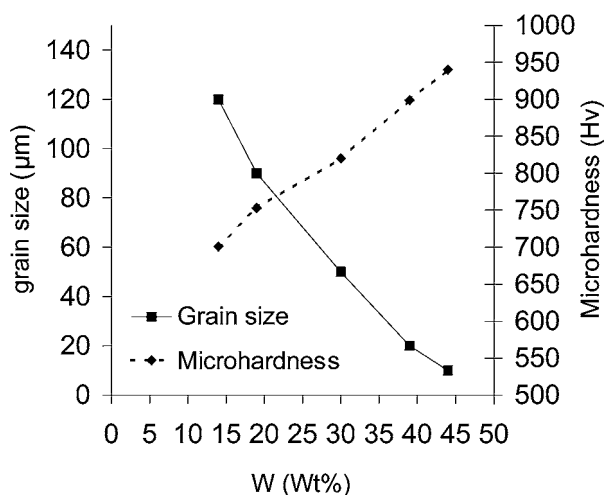


Figure 10 Evolution of grain size and microhardness with tungsten concentration.

content. As can be seen, the highest tungsten content yields to the hardest alloys, with the lowest grain size.

4. Discussion

Sintering of tungsten has been studied by several authors in the past. Hayden and Brophy [8], Brophy *et al.* [9] have determined the activation energies for sintering tungsten with several activators. They showed that its value was maximum with ruthenium activator (477 kJ/mol), whereas it was minimum with nickel. This confirms our observation that ruthenium is a bad activator, which leads to heterogeneous alloys.

TABLE VII Influence of Mo/W ratio

	Process	Theoretical density ($\text{g} \cdot \text{cm}^{-3}$)	Apparent density ($\text{g} \cdot \text{cm}^{-3}$)	Grain size (μm) $\pm 10\%$	(Hv) $\pm 2\%$
Mo/W = 3 Cr ₃₉ Mo ₄₅ W ₁₅ Pd ₁	High pressure sintering heated 24 hours at 1600°C	9.34	9.25	120	701
Mo/W = 2 Cr ₃₉ Mo ₄₀ W ₂₀ Pd ₁	High pressure sintering heated 24 hours at 1600°C	9.55	9.5	90	753
Mo/W = 1 Cr ₃₉ Mo ₃₀ W ₃₀ Pd ₁	High pressure sintering heated 24 hours at 1600°C	9.98	9.9	50	820
Mo/W = 1/2 Cr ₃₉ Mo ₂₀ W ₄₀ Pd ₁	High pressure sintering heated 24 hours at 1600°C	10.45	10.3	20	899
Mo/W = 1/3 Cr ₃₉ Mo ₁₅ W ₄₅ Pd ₁	High pressure sintering heated 24 hours at 1600°C	10.70	10.5	10	940

Samsonov and Jakowlev [10] observed that sintering of tungsten at 1400°C with 0.30% Ni led to a grain size larger than 100 μm , while substitution of nickel with ruthenium or palladium led to a grain size smaller than 30 μm . However, because of the high activation energies for sintering with ruthenium, the experiments with this element had been done at a higher temperature (1700°C).

Relative to the influence of nickel as an activator, considering the binary Mo-Ni and Ni-Cr phase diagrams, the formation of a liquid phase containing Ni, Mo and Cr cannot be excluded. Indeed, referring to literature (Rabkin *et al.* [11], Glebovsky *et al.* [12] and Penisson *et al.* [13]), it has been shown that the formation of a liquid layer can explain the wetting of the grain boundaries of molybdenum.

No experimental evidence of the appearance of such a liquid phase has occurred. Moreover, the kinetic of the sintering process is governed by solid state diffusion, as shown by Fig. 3a. This behaviour is similar to that of tungsten sintered with Ni as an activator agent. In this case, Hayden and Brophy [8] and Brophy *et al.* [9] have observed that the grain size of tungsten sintered with Ni was inversely proportional to the nickel content. The important difference between the diffusion coefficients of Cr, Mo or W in nickel [14] ($D_{\text{Cr}} \gg D_{\text{Mo}} \gg D_{\text{W}}$ in Ni) allows to assume that chromium first diffuses in nickel to form a NiCr phase. As for “pure” tungsten [15], sintering of MoWCr alloys activated by nickel is thus probably governed by solid state diffusion. Addition of a small amount of nickel to refractory metals is known to affect the surface structure of tungsten grains and consequently the grain boundary structure of the sintered samples [13, 16, 17]. Brophy *et al.* [18] and Sakamoto *et al.* [19]. observed that one monolayer of nickel coating on tungsten particles is sufficient to support high diffusion of tungsten through or on the nickel, thereby forming the interparticle necks. Nickel thus induces a significant increase in the rate of densification by grain boundary diffusion. Thus a significant decrease of the grain size for the MoWCr alloys occurred with increasing nickel content.

As regards the influence of nickel on the microhardness, it can be supposed that nickel contributes to softening of the very hard refractory alloy matrix by a solid solution mechanism. However, comparing the respective influences of chromium and nickel from this point of view, it seems very likely that in the case of sintering

with Ni, the microhardness values are more affected by the structure (grain size) of the alloys than by the dissolution of nickel in the matrix.

With palladium as the activating agent, sintering results mainly from the formation of a Cr- and Pd-rich phase (“CrPd”), which is molten at the fabrication temperature of the alloys. Sintering is thus activated by this liquid phase, which forms temporarily, until palladium dissolves into the α -MoWCr matrix. Contrary to nickel, sintering with palladium is thus activated by diffusion of chromium, molybdenum and tungsten through a liquid “CrPd” phase wetting the metal grains. The size of the alloy grains thus depend upon the volume fraction of the “CrPd” phase, which forms during sintering. This fraction increases as the solubility of palladium in the refractory alloy decreases, i.e., when the Cr content is low.

Consequently, alloys with 19 wt% Cr have a larger grain size than 40 wt% Cr alloys. For chromium contents higher than 40 wt%, the grain size increases with the concentration of chromium, because this element increases the rate of diffusion of all elements in the ternary alloy. Above 40 wt% Cr, addition of chromium should thus lead to a progressive transition from liquid phase to “diffusion” sintering.

As regards microhardness evolution with the chromium content of the alloys sintered with palladium, a continuous evolution can be observed. This can be ascribed to the substitution of the hard elements Mo and W by chromium in the α MoWCr solid solution. For low Cr alloys, a question arises about the possible influence of the α CrPd phase which subsists at the grain boundaries. Due to the very low volume fraction of this phase and also to the small size of its precipitates, no visible effect could be observed on the microhardness measurements.

Concerning the Mo/W ratio, for a constant Cr and Pd level, enrichment of the alloys with tungsten leads to a smaller grain size and high microhardness values. This result can be explained by the very high melting point of tungsten, which significantly decreases the volume diffusion of all alloying elements proportionally to its content. The method of synthesis also induces significant differences in the alloy properties. The microhardness of an alloy prepared by pressure-assisted sintering is higher than that of the same alloy composition prepared with natural sintering (Fig. 8). This difference results from a higher level of stress accumulation

during high pressure sintering, which cannot be completely released during the homogenisation annealing. Differences between the microhardness values of alloys synthesised with and without mechanical alloying follow the same trend. Moreover, as confirmed by the widening of the diffraction lines, MA decreases the particle size of the metal powders with consequences for the microstructure of the alloys.

5. Conclusion

The microstructure of MoWCr alloys has been studied over a broad range of compositions. Syntheses of these materials have been carried out by techniques based on natural sintering, uniaxial-pressure-assisted sintering, or mechanical alloying followed by uniaxial-pressure assisted-sintering. Homogeneous and dense alloys can only be obtained by uniaxial-pressure assisted-sintering, with use of nickel or palladium as the activator.

Liquid phase sintering is observed with palladium, with the formation of a chromium/palladium-rich molten phase, which wets the metal grains. In the presence of nickel, sintering is activated via diffusion, probably through a nickel-rich surface layer formed on metal grains.

The synthesis process has a significant influence on the microstructure of the alloys as well as on their hardness. Uniaxial-pressure-assisted-sintering generates stresses which increase the microhardness of the alloys prepared with this method.

For given synthesis parameters, tungsten and molybdenum levels have also a great influence on the grain size and microhardness of the alloys. Increasing the concentration of tungsten, the hardest and most refractory component, leads to a finer grain size (lower diffusion rate) and harder alloys.

References

1. D. S. EVANS, in High Temperature Materials, 6th Plansee Seminar (Metallwerk Plansee, Austria, 1968).
2. I. YA. DZYKOVICH, V. V. PANICHKINA, V. V. SKOROKHOD and L. I. SHAIKIDMAN, *Poroshk Metall.* **158**(2) (1976) 86.
3. D. LEE and G. SIMKOVICH, *Oxid. Met.* **34**(1/2) (1990) 13.
4. *Idem.*, *ibid.* **31**(3/4) (1989) 265.
5. *Idem.*, *J. Less-Com. Met.* **163** (1990) 51.
6. *Idem.*, *ibid.* **169** (1991) 19.
7. C. W. CORTI, *Plat. Met. Rev.* **4**(30) (1986) 184.
8. H. W. HAYDEN and J. H. BROPHY, *J. Electrochem. Soc.* **110**(7) (1963) 805.
9. J. H. BROPHY, L. A. SHEPARD and J. WULFF, in "Powder Metallurgy," edited by W. Leszinski (AIME-MPI, Interscience, New York, 1961) p. 113.
10. G. W. SAMSONOV and W. I. JAKOWLEV, *Z. Metallkd.* **62**(8) (1971) 621.
11. E. RABKIN, D. WEYGAND, B. STRAUMAL, V. SEMENOV, W. GUST and Y. BRECHET, *Phil. Mag. Letters* **73** (1996) 187.
12. V. GLEBOVSKY, B. STRAUMAL, V. SEMENOV, V. SURSAEVA and W. GUST, in Proc. 13th Plansee Seminar, edited by H. Bildstein and R. Eck (Metallwerk Plansee, Reutte, 1993) Vol. 1, p. 429.
13. J. M. PENISSON and T. VYSTAVEL, *Acta Mater.* **48** (2000) 3303.
14. E. A. BRANDES and G. B. BROOK (eds.) "Smithell Metals reference book," 7th edn. (1992).
15. A. BELHADDJHAMIDA and R. M. GERMAN, in "Tungsten and Tungsten Alloys, Recent Advances," edited by A. Crowson and E. S. Chen (TMS Pub, 1991) p. 3.
16. N. M. HWANG, Y. J. PARK, D. Y. KIM and D. Y. YOON, *Acta Metall.* **42**(5) (1999) 421.
17. J. M. PENISSON and T. VYSTAVEL, *Acta mater.* **48** (2000) 3303.
18. T. SAKAMOTO, T. HONDA, H. MIURA and K. OKAZAKI, *Met. Trans. JIM* **38**(4) (1997) 326.
19. J. H. BROPHY, H. W. HAYDEN and J. WULFF, *Trans. Met. Soc. AIME* **224** (1962) 797.

Received 24 April 2001

and accepted 24 January 2002